

Supporting Information

Elucidating the Molecular Mechanism of Noncompetitive Inhibition of Acetylcholinesterase by an Antidiabetic Drug Chlorpropamide: Identification of New Allosteric Sites

Abhinandan Das[‡], Krishnendu Sinha[‡] and Suman Chakrabarty*

Department of Chemical and Biological Sciences, S. N. Bose National Centre for Basic Sciences,
JD Block, Sector III, Salt Lake, Kolkata 700106, India.

[‡] These authors have contributed equally.

* To whom correspondence should be addressed: sumanc@bose.res.in

Table S1: List of residues present in the different sites as visualized in the Figure 1

Site	List of residues
CAS	S203, E334, H447
PAS	Y72, D74, Y124, E285, W286, Y341
Allosteric Site	L373, A374, A377, H381, F531, R534, F535, K538, L539, A542

Table S2: List of residues for five major ligand binding sites as shown in Figure 2

Ligand Binding Sites	Residue Numbers
Site-1 (Allosteric Site)	372-390, 525-543
Site-2	138-145, 460-490
Site-3	4-20, 105-112, 182-190
Site-4	240-255, 290-300
Site-5	355-370

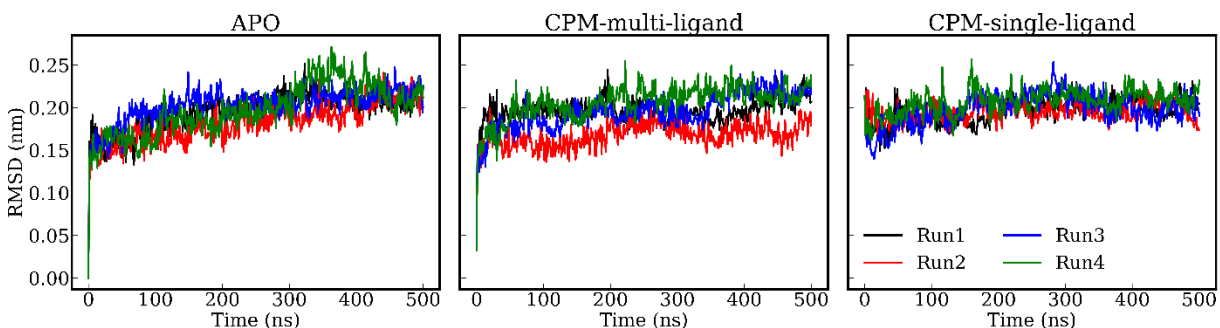


Figure S1: Backbone Root Mean Square Deviation (RMSD) plots for the Apo, CPM-multi-ligand, and CPM-single-ligand systems over 500 ns of simulation. Four independent simulation runs are shown for each system. The RMSD values remain around 0.2 nm across all systems, indicating structural stability throughout the simulation.

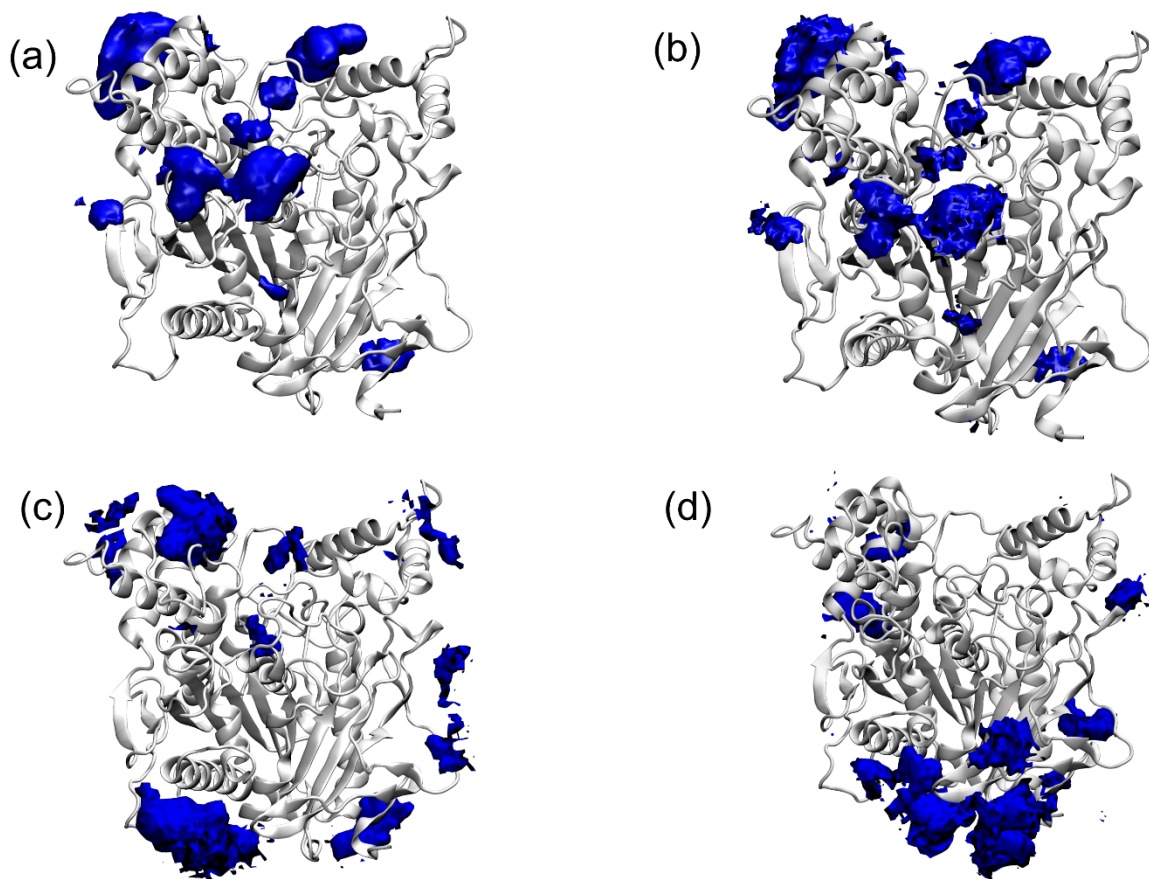


Figure S2: Spatial Density Function (SDF) of CPM ligand around AChE for four independent simulations of the multi-ligand setup. In most cases, there is a significant population of ligands around the C-terminal allosteric site.

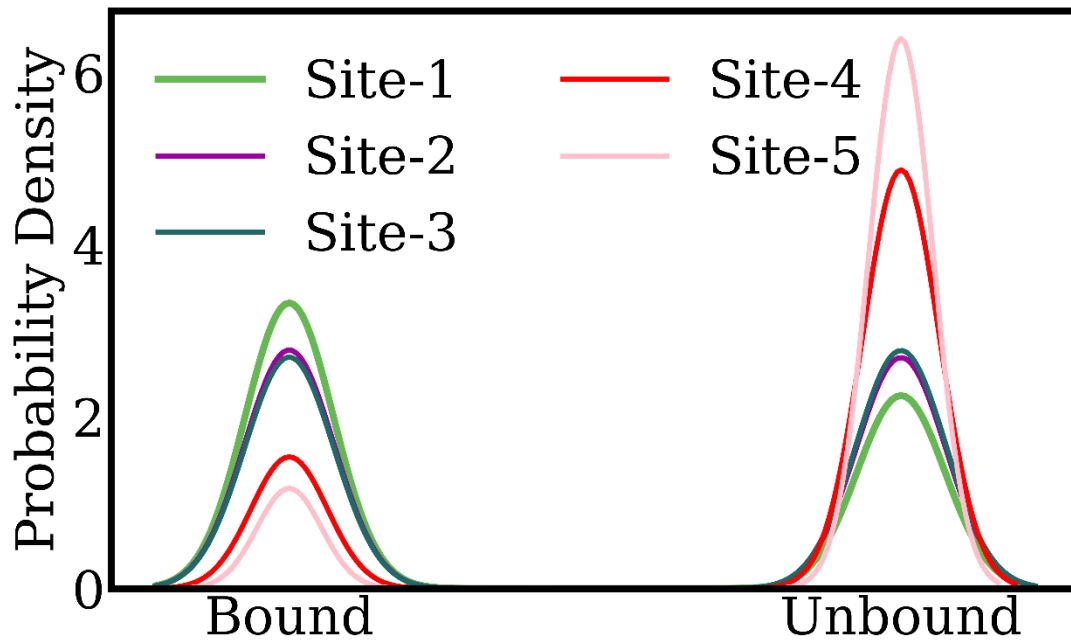


Figure S3: Probability density distribution of CPM ligands in the "bound" and "unbound" states across five identified binding sites, showing the highest binding propensity at Site-1.

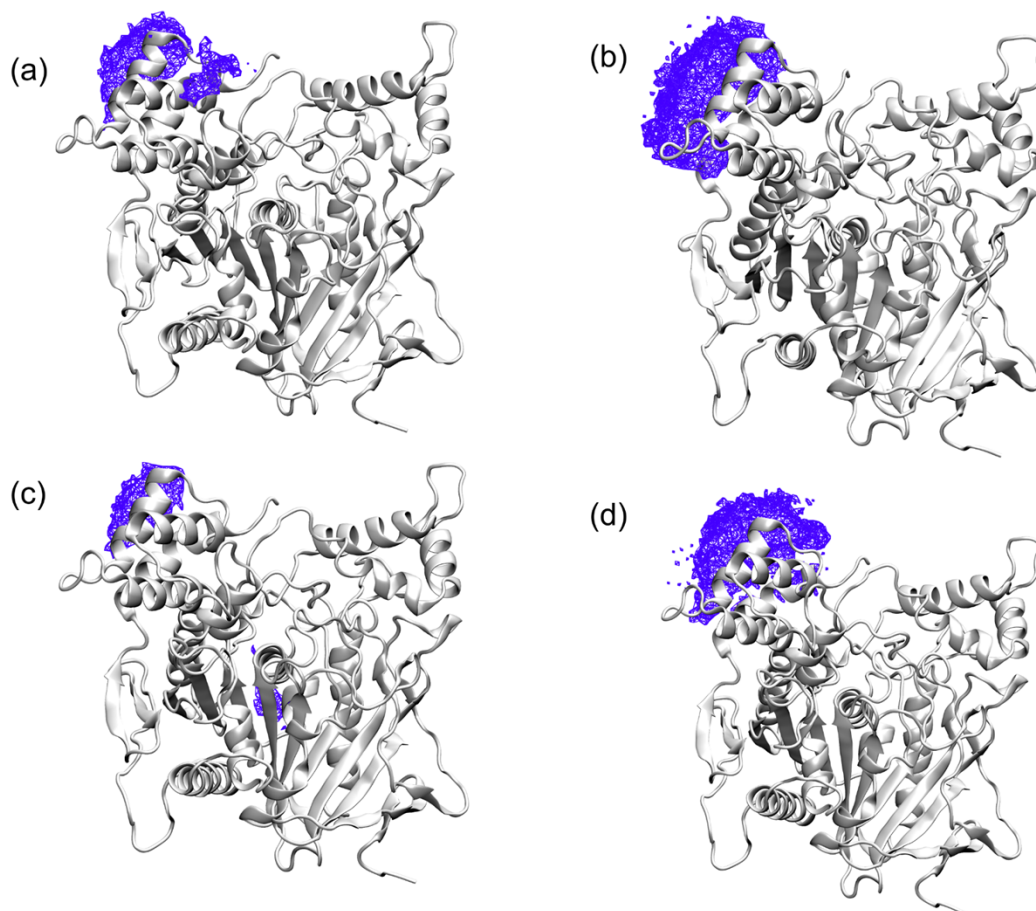


Figure S4: Spatial Density Function (SDF) of CPM single ligand system for four independent trajectories. For all cases, the ligand stays in the C-terminal allosteric site which suggests this is a stable binding site within the simulation timescale of 500ns.

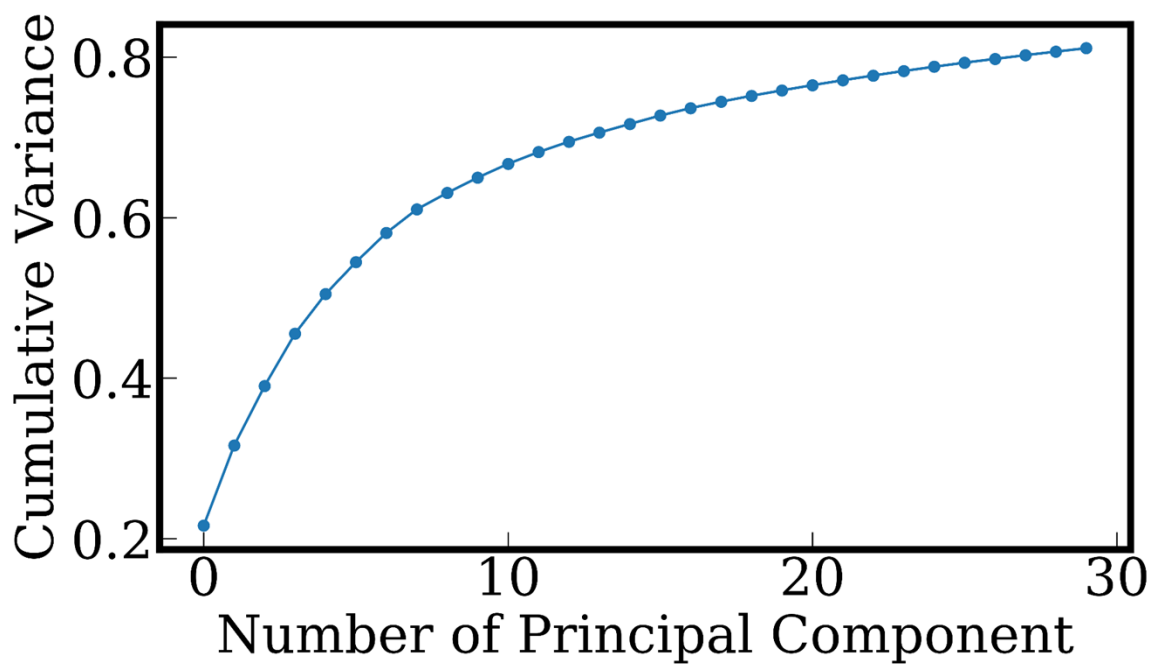


Figure S5: Cumulative variance of PCA analysis. The first 30 principal components account for 80% of the motion.

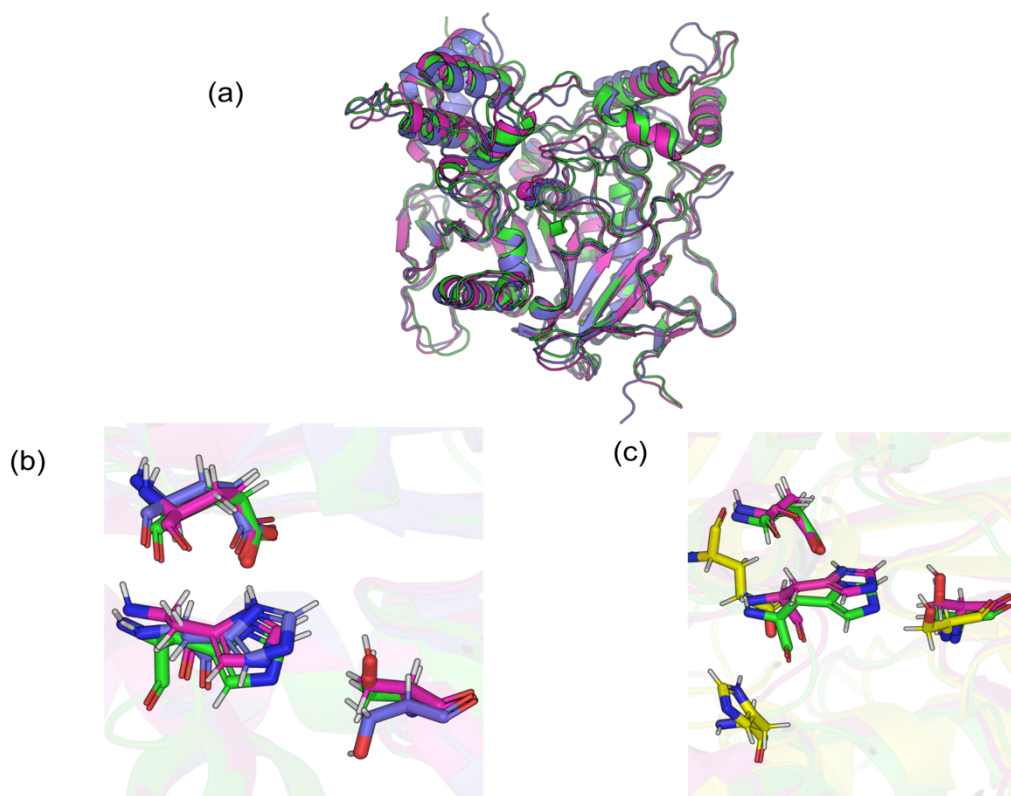


Figure S6: Superimposition of various combinations of clusters as obtained from the probability distribution of (PC1, PC2) space as shown in Figure 5. (a) Cluster A, Cluster B, and Cluster C have similar PC2 values but different PC1 values. Comparison of the representative structures from these two clusters, we find that PC1 describes a global motion. The structural changes between these states are in the C-terminal region, PAS region and different loops of the protein structure. (b) comparison of CAS region for these clusters (A, B and C) show almost no change in the structure of the catalytic triad confirming PC1 does not involve the CAS. (c) Superposition of the CAS region for clusters A, B, and D. We see that for cluster D (with higher PC2 value), there is a significant change in the CAS region. Thus we can safely conclude that PC2 describes a more local motion near the active site. Clusters A, B, C and D are shown in green, magenta, blue, and yellow color, respectively.